Nanoscale

RSC Publishing

PAPER

View Article Online
View Journal

Unimolecular amplifier: principles of a three-terminal device with power gain†‡

Cite this: DOI: 10.1039/c3nr00956d

Cormac Toher,§[a] Daijiro Nozaki,[a] Gianaurelio Cuniberti[ab] and Robert M. Metzger*[ab]

A single molecule composed of three linked moieties can function as an amplifier of electrical current, when certain conditions are met by the molecular orbitals of the three component parts. This device should exhibit power gain at appropriate voltages. In this work, we will explain a plausible mechanism by which this device should work, and present its operating characteristics. In particular, we find that a fundamental requirement for current amplification is to have the LUMO of the central moiety more strongly coupled to a control electrode than it is to the other orbitals in the molecule, while the HOMO of this moiety should be more strongly coupled to the orbitals in the other moieties than it is to the control electrode.

Received 23rd February 2013
Accepted 4th June 2013

DOI: 10.1039/c3nr00956d

www.rsc.org/nanoscale

Published on 06 June 2013. Downloaded by Osaka University on 25/06/2013 05:50:09.

Introduction

Molecular Electronics[1] started with a seminal paper by Aviram and Ratner (AR),[2] which proposed a one-molecule rectifier of electrical current. Much progress has been made in realizing unimolecular rectification[3,4] and in measuring the electrical conductivity of single molecules and monolayers.[5–7] Multi-terminal logic gates have also been proposed.[8] For molecular electronics at the 2 nm scale to become technologically useful, it must have not only passive devices (resistors, capacitors and rectifiers), but also active devices that can controllably deliver power gain. Almost forty years after AR, we now propose an electroactive molecule with power gain, the unimolecular equivalent of a vacuum-tube triode (VTT) or a bipolar junction transistor (BJT): we will call it a unimolecular amplifier (UA). The UA idea has been mentioned briefly elsewhere;[9] we now buttress the idea with realistic theoretical calculations. We differentiate the behavior of UA from the well-established use of bulk organic semiconductors and even organic monolayers or carbon nanotubes as the active elements in field-effect transistors (FETs).[10] Theoretical attention has also been devoted to three-terminal molecular transistors, which are based on quantum interference effects.[11] However, as explained below, the UA is definitely NOT simply an FET and operates *via* a different mechanism. As we see it, the UA will consist of a molecule with three "electroactive" components or moieties, covalently linked into a single molecule, and each connected by a covalent bond to a separate metal electrode, as shown in Fig. 1.

The idea is simple: an organic electron acceptor moiety A (which, as an isolated molecule, has a relatively large electron affinity) is covalently coupled to an electron donor moiety D1 (which, as an isolated molecule, has a relatively small ionization potential) and is also covalently coupled to a second electron donor moiety D2 (with a moderate ionization potential). The current path through the molecule depends on the alignment and occupation of the molecular levels of the different moieties. This in turn can be adjusted by applying a voltage to the electrode attached to the central moiety, allowing for control over the total current through the device.

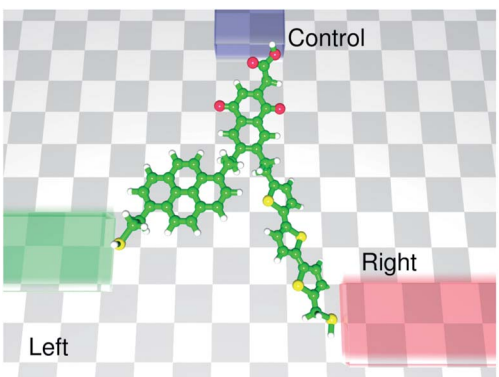

Fig. 1 Conceptual structure of a unimolecular amplifier: covalently attached to the (left) Au electrode by a thiolate linkage is the donor D1 (pyrene); covalently attached to the (right) Au electrode through a thiolate linkage is the donor D2 (terthiopene); attached to the (center) Al electrode by a carboxylate linkage is the acceptor A (napthoquinone). The atomic arrangement in the electrodes is deliberately left imprecise.

[a]*Institute for Materials Science, Max Bergmann Center of Biomaterials, Dresden University of Technology, 01062 Dresden, Germany. E-mail: research@nano.tu-dresden.de; rmetzger@ua.edu*

[b]*Laboratory for Molecular Electronics, Chemistry Department, University of Alabama, Tuscaloosa, AL 35487-0336, USA*

† Electronic supplementary information (ESI) available. See DOI: 10.1039/c3nr00956d

‡ R. M. M. wishes to dedicate this paper to his research advisor, Prof. Harden Marsden McConnell, who celebrates his eighty-sixth birthday on 18 July 2013.

§ Present address: Department of Mechanical Engineering and Materials Science, Duke University, Durham, NC 27708, USA.

Published on 06 June 2013. Downloaded by Osaka University on 25/06/2013 05:50:09.

This phenomenon would be analogous to what happens in a VTT (where the grid-to-plate back-bias (*i.e.* its electric field) can control the anode-to-plate current) or in a npn' BJT (where the base-to-collector back bias and the resultant base-to-collector current can control the emitter-to-collector current).

At very short distances (*e.g.* 1 to 6 Å) between any two metal electrodes there is a significant quantum-mechanical tunneling current, even in vacuum, that is equal (*i.e.* symmetrical) in both directions. This through-space[12] tunneling current decays exponentially with distance; at larger distances it becomes very small.

Unimolecular rectifiers (molecules about 20 Å long between metal electrodes) show a clear asymmetry in the measured currents, both in single molecules[13] and in monolayers.[3]

One issue is whether such asymmetric currents are really "through-bond",[12] in which case they either transfer some of their energy into exciting molecular vibrations (inelastic tunneling)[14,15] or else involve resonance with an available molecular orbital (elastic "orbital-meditated tunneling").[15,16]

As expected, a calculation has shown that resonance with accessible molecular orbitals does enhance the current, relative to the non-resonant case: the density of states, and therefore the transmission factor, become relatively large.[17] However, the amplitude of the molecular wavefunction must also be significant in close proximity to the electrode, and a molecular orbital that is not close in energy to the LUMO can also contribute significantly to the local density of states.[17]

Recent progress in synthetic chemistry (in particular the Sonogashira coupling reaction, which creates acetylene bridges, or the Suzuki coupling, which makes ethane bridges) makes the design of a UA molecule realistic.

The experimental challenge, on which we are working concurrently, is to fabricate three metal electrode tips, with a separation of 2 nm from each other, which can probe adequately the electrical properties of UA; to our knowledge, this has not yet been realized anywhere. There already are at least three known ways of establishing a nanogap between two electrodes (mechanical break junction, electromigration break junction, and scanned probe junction);[18–21] in contrast, making three (or four) electrodes within 2 nm of each other is a difficult goal we hope to achieve experimentally.

This work is composed of two main parts. In the first part, we use DFT-based calculations to investigate the electronic structure properties of three-terminal molecular devices. This includes comparing the energies of the frontier orbitals of different molecules, which may function as unimolecular amplifiers, and investigating the strength of the coupling between these orbitals and the electrodes.

In the second part, we will use model electron transport calculations to show how, and when, a molecule can deliver power gain. We also determine under which conditions and to what extent the control electrode works through an electric field effect (in which case the UA would be a simple FET), and under which conditions and to what extent it works as the result of electrostatic charging.

While DFT calculations are used to obtain reasonable starting values for some of the parameters in this model, this work is not intended to be a quantitative description of an actual device. Instead, our intention is to demonstrate how a such a molecular amplifier may work, and to determine the value range of electronic properties that will deliver power gain.

Three-terminal molecules

We initially considered four molecules (UA1 to UA4) (Fig. 2). In UA1 and UA3 the linkages throughout the central part of the molecule are aromatic, whereas in UA2 and UA4 the linkages are interrupted by four aliphatic (saturated) carbon atoms (Y and Z). These four molecules were designed from the "strong" electron donor tetrathiafulvalene (T), which has an ionization potential of 6.83 eV (ref. 22) and the "moderate" electron donor pyrene (P), which has a larger ionization potential of 7.41 eV.[23] UA1 and UA2 use the strong electron acceptor dicyanoquinodiimine, which has an electron affinity of 3.3 eV,[24] while UA3 and UA4 use the weaker electron acceptor benzoquinone, which has an electron affinity of 1.9 eV.[25]

The electronic properties of each of these molecules were calculated using the DFTB+ code.[26] For the determination of the stable configurations of the molecules, we first performed a geometry optimization by means of the conjugated-gradient technique with the DFTB+ code. The geometry optimization was carried out until the absolute value of the interatomic force was reduced to less than 10–4 atomic units. For the basis sets we used the Slater–Koster (SK) parameters developed by Elstner *et al.* for the C, H, N, O atoms[27] and those of Niehaus *et al.* for

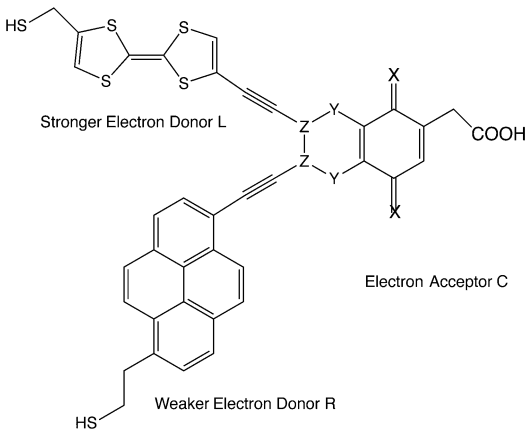

UA1: X=NCN (C is strong acceptor), Y=CH, Z=C (aromatic link);
UA2: X=NCN (C is strong acceptor), Y=CH_2, Z=CH (aliphatic link);
UA3: X=O (C is weak acceptor), Y=CH, Z=C (aromatic link);
UA4: X=O (C is weak acceptor), Y=CH_2, Z=CH (aliphatic link)

Fig. 2 Four model molecules (UA1 to UA4) for a unimolecular amplifier: in UA1 and UA3 the linkages throughout the central part of the molecule are fully aromatic, while in UA2 and UA4 the linkages are interrupted by four aliphatic saturated carbon atoms. All four molecules were designed from the "strong" electron donor tetrathiafulvalene (T) (smaller ionization potential I_D) and the "moderate" electron donor pyrene (P) (larger ionization potential I_D). UA1 and UA2 use the strong electron acceptor dicyanoquino-diimine, whose electron affinity A_A matches that of TCNQ (7,7,8,8-tetracyanoquinodimethan: larger electron affinity A_A), while UA3 and UA4 use the weaker electron acceptor benzoquinone (smaller electron affinity A_A).

This journal is © The Royal Society of Chemistry 2013

Published on 06 June 2013. Downloaded by Osaka University on 25/06/2013 05:50:09.

the S atoms.[28] Molecules UA1 through UA4 were designed from known organic one-electron donor and acceptor molecules. Polarization will reduce considerably the HOMO–LUMO gap from the estimates available for the differences ($I_D - A_A$): this reduction may be as large as 2 eV. Also, it is well known that DFT-based calculations systematically underestimate the size of the HOMO–LUMO gap. The disappointing results are relegated, with a discussion, to Table A of the ESI:† the ethynyl linkages intermingled electron densities across the conceptually distinct moieties, and the computed orbital energies obtained did not work well with the algorithms introduced below.

Since the initially proposed molecules did not have the required properties, we calculated two more molecules (UA5 and UA6) shown in Fig. 3, one of which is asymmetric and the other symmetric. For the asymmetric molecule UA5, the strong electron donor moiety is a thiophene trimer, the weak electron donor moiety is pyrene, and the electron acceptor moiety is naphthoquinone. For the symmetric molecule, both donor moieties are based on thiophene trimers. The moieties are linked by saturated aliphatic chains, and the molecular orbitals are confined to the individual moieties. Molecules UA5 and UA6 do have the required properties, with the HOMO on the thiophene and the LUMO on the central acceptor, as shown in Table 1. The results of these calculations were checked against DFT calculations using the SIESTA program.[29]

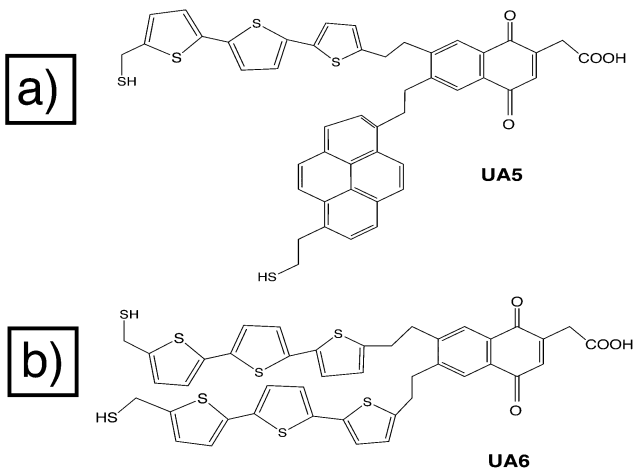

Fig. 3 Two molecules (UA5 and UA6) which produce the required properties for the unimolecular amplifier, according to DFTB+ calculations: (a) asymmetric molecule, UA5, with a strong electron donor is based on a thiophene trimer, a weak electron donor based on pyrene, and an electron acceptor based on naphthoquinone. (b) Symmetric molecule UA6, with two strong electron donors based on thiophene trimers, and an electron acceptor based on naphthoquinone.

Table 1 Molecular orbital energies (in eV) for the different parts of the molecules shown in Fig. 3. The wave function for each orbital was plotted in real space in order to determine which moiety it was on

	Asymmetric (UA5)		Symmetric (UA6)	
Level	HOMO	LUMO	HOMO	LUMO
ε_L	−5.531	−3.033	−5.005	−2.84
ε_C	−5.929	−3.945	−5.931	−3.95
ε_R	−5.008	−2.833	−5.005	−2.84

Three-terminal transport model

In order to investigate the behavior of a unimolecular amplifier under different conditions, we used a simple model based on that introduced by Paulsson *et al.*[30] for electronic transport in molecular junctions. The aim of this model is to demonstrate in a qualitative way how such a device would work, as well as to understand the physical regimes in which such a device would operate. However, it should be understood that some aspects of this model may be oversimplified, and that some results may be artifacts due to the limitations of the model. Such limitations will be noted where applicable.

We could have resorted to a more elegant but laborious approach using non-equilibrium Green's functions (NEGF) to compute the elastic current within the Landauer–Büttiker–Keldysh formalism.[6,31–34] This would combine pictures of molecular orbital amplitudes, electrode geometries, and the tunneling current under the conditions of resonance transfer to and from precisely modeled metal electrodes.[35–39] This was not done, partly because much does depend on the choices of the Au or Al cluster geometries (and experiments[40] and theory tend to disagree), and partly because the molecules computed in the previous section are very large.

The reasons for choosing a simple model include the difficulty of realistically describing the real-space potential generated by three electrodes at different bias, which are aligned at different angles, as well as the ease of altering the parameters, so as to investigate different regimes. Additionally, many of the shortcomings of this model will also be present in *ab initio* DFT-based transport calculations[41,42] using approximate exchange-correlation potentials such as LDA or GGA.[43–46]

The unimolecular amplifier consists of three parts or moieties (connected by σ-bonds), which are labelled L (left), C (center or control), and R (right). Each of these parts is modeled by two energy levels ε_a (where a runs over L HOMO, L LUMO, *etc.*), which are connected both to the other parts of the molecule and to an electrode, as shown in Fig. 4.

Strictly speaking, the labels HOMO or LUMO are valid for one-electron levels of a molecule, and used here for components

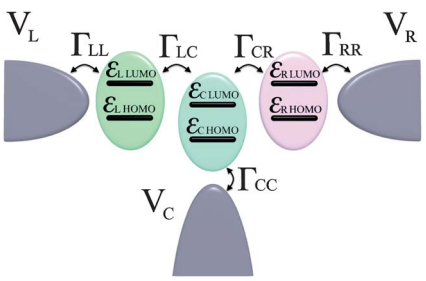

Fig. 4 Simple model for unimolecular amplifier. Each molecular component (moiety) is modelled by two electronic levels, a HOMO level and a LUMO level, with energies ε_a. The rate at which electrons can move between these molecular orbitals and the electrodes and between moieties is described by a set of coupling constants Γ.

Published on 06 June 2013. Downloaded by Osaka University on 25/06/2013 05:50:09.

or moieties of a molecule separated from the other moieties by sufficiently long σ-bonds. Also, the HOMO or LUMO for an isolated molecule are not the same things as the energy levels in a transport model of a molecule connected to electrodes as infinite sinks: in transport, one should use the terms "ionization level" instead of HOMO and "affinity level" instead of LUMO.[47]

The electrodes are modeled as electron reservoirs with a constant density of states (wide-band approximation), and are also labelled L, C and R, according to which component of the molecule they are connected to.

The states in the electrodes are populated according to the Fermi distribution $f(E, \mu)$, where μ is the chemical potential which can be altered to simulate the effect of an applied bias. The rate at which the electrons can move between the electrodes and the molecular levels, or between the different molecular levels in the molecule, are described by a set of coupling constants Γ_i, where $\Gamma_i/\hbar$ is the rate at which electrons cross the tunnel barrier at junction i. Each electrode j (where j is one of L, C or R) will attempt to impose an occupation N_{ja} onto each molecular level a, where $N_{ja} = 2f(\varepsilon_a, \mu_j)$. The current I_{ja} between the electrode j and the level a will be determined by the difference between the occupation which the electrode is trying to impose, N_{ja}, and the actual occupation of the molecular level N_a, so that:

$$I_{ja} = \frac{e\Gamma_{ja}}{\hbar}\left(N_{ja} - N_a\right) \quad (1)$$

Note that the sign convention is chosen so that the current is positive for $N_{ja} > N_a$ and negative for $N_{ja} < N_a$. Thus, in the results, a positive value for a current through a particular electrode-molecule interface means that electrons are entering the molecule through this interface, and a negative value means electrons are exiting through this interface.

In order to account for the broadening of the molecular orbitals due to the interactions with the electrodes, each molecular energy level ε_a is described by a Lorentzian density of states, $D_a(E)$:

$$D_a(E) = \frac{1}{2\pi}\frac{\Delta_a}{(E - \varepsilon_a)^2 - (\Delta_a/2)^2} \quad (2)$$

where Δ_a is the broadening of the molecular level ε_a due to the interaction with the electrodes, and in general $\Delta_a = \sum_j \Gamma_{ja}$. The occupation which the attached electrode attempts to impose on this molecular orbital, N_{ja}, is thus now given by an integral over the energy weighted by the relevant Fermi distribution:

$$N_{ja} = \int D_a(E) f(E,\mu_j) \mathrm{d}E \quad (3)$$

Within the molecule, levels will also attempt to impose different occupations on each other, depending on both their occupation and their relative energies. If level a is above level b, so that $\varepsilon_a > \varepsilon_b$ then if level a is not completely empty (*i.e.* if $N_a > 0$) and level b is not completely filled (*i.e.* $N_b < 2$), then charge from level a will be transferred to level b, so that either level b is now fully occupied or level a is fully empty. Therefore, the occupation that level a tries to impose on level b, N_{ab}, for $\varepsilon_a > \varepsilon_b$ is given by:

$$N_{ab} = (N_a + N_b) \text{ if } (N_a + N_b) \leq 2;\ N_{ab} = 2 \text{ if } (N_a + N_b) > 2. \quad (4)$$

Similarly, the occupation that level b tries to impose on level a, N_{ba}, for $\varepsilon_a > \varepsilon_b$ is given by:

$$N_{ba} = 0 \text{ if } (N_a + N_b) \leq 2;\ N_{ba} = N_a - (2 - N_b) \text{ if } (N_a + N_b) > 2. \quad (5)$$

The current I_{ab} between the level a and the level b will be determined by the difference between the occupation which level a is trying to impose on level b, N_{ab}, and the actual occupation of the level, N_b:

$$I_{ab} = \frac{e\Gamma_{ab}}{\hbar}(N_{ab} - N_b) \quad (6)$$

If the device is in the steady-state condition, then the occupation of each level is constant, so that the sum of all of the currents in and out of this level must be equal to zero. For level a, this gives:

$$\sum_j I_{ja} + \sum_b I_{ba} = 0 \quad (7)$$

Inserting the expressions from eqn (1) and (6) into eqn (7) gives:

$$\sum_j \frac{e\Gamma_{ja}}{\hbar}\left(N_{ja} - N_a\right) + \sum_b \frac{e\Gamma_{ba}}{\hbar}(N_{ba} - N_a) = 0 \quad (8)$$

Rearranging and simplifying gives an expression for the steady-state occupation of the level:

$$N_a = \frac{\sum_j \Gamma_{ja} N_{ja} + \sum_b \Gamma_{ba} N_{ba}}{\sum_j \Gamma_{ja} + \sum_b \Gamma_{ba}} \quad (9)$$

The molecular energy levels ε_a are not fixed. Instead, their value depends on both their occupation N_a and on the local applied electric field. Since this model does not directly consider the actual geometry of the system, the effect of the electric field is included by considering the net bias applied to the different electrodes. The equation for the molecular level energy thus becomes:

$$\varepsilon_a = \varepsilon_{a0} + U_a\,(N_a - N_{a0}) + U_{ja}^{\mathrm{ee}}\,(\mu_j - \mu_{j0}) \quad (10)$$

where U_a is the energy by which the molecular level a changes when an electron is added to or removed from it, and U_{ja}^{ee} is the energy by which the molecular level a changes in response to the electric field created by the voltage applied to electrode j. Values for these parameters were obtained from DFT calculations as described below. Note that, strictly speaking, such behavior is only valid in the limit of strong coupling to the electrodes. This approximation does not take into account the type of strong correlation effects associated with the strong electron localization, which occurs in the weak-coupling regime. In particular, it will share many of the same problems present in approximate exchange-correlation functionals, such

 This journal is © The Royal Society of Chemistry 2013

Published on 06 June 2013. Downloaded by Osaka University on 25/06/2013 05:50:09.

as LDA or GGA.[43–46] The parameter μ_{j0} is the chemical potential of the electrode j at zero bias, and for all of the calculations described here is set to −5.0 eV.

In the calculation described in the next section, we will consider two different cases: the first where only elastic electron transport occurs, and the second where both elastic and inelastic transport occur. To model elastic transport, an additional restriction was imposed, so that electrons could only move between orbitals which are close in energy. This was done by multiplying the coupling constant between two orbitals by a factor, which depended on the overlap of the DOS of these orbitals, as follows:

$$\Gamma'_{ab} = \Gamma_{ab} \int \sqrt{D_a(E) D_b(E)} \mathrm{d}E \quad (11)$$

where $D_a(E)$ and $D_b(E)$ are normalized. If $\varepsilon_a = \varepsilon_b$, then, because all of the orbitals have the same broadening, $D_a(E) = D_b(E)$, and the result becomes an integral over $D_a(E)$, which is equal to one, and thus $\Gamma'_{ab}(E) = \Gamma_{ab}$. For the case where inelastic transport is allowed, *i.e.* where electrons can lose energy by scattering and thus transfer into lower energy orbitals, this restriction was removed.

Once the steady-state occupation of each level has been calculated self-consistently, the total current across any interface between the molecule and the electrodes or between parts of the molecule can be easily calculated by summing over the appropriate values obtained from eqn (1) or (6), respectively.

Eqn (1)–(11) were converted into a 500-line *ad hoc* FORTRAN computer source program with a graphic input/output interface for a PC microcomputer.

Transport model parameters

The molecular orbital energy values were taken from Table 1. We estimated the charging energy U_a of the molecule by comparing the energies of the HOMO and LUMO levels of the neutral molecule with those of the molecule having a single extra electron. The shift of the energy levels of each part of the molecule due to an applied external electric field was also calculated to obtain values for the parameter U_{ja}^{ee}. Using the results of these calculations, values for $U_a = 4.0$ eV and $U_{ja}^{ee} = 0.3$ eV were decided on.

The values for the coupling between the different parts of the molecule, Γ_{ba}, and between the molecule and the electrodes, Γ_{ja}, were varied, so as to tune the size of the currents between the different orbitals, and thus optimize the functioning of the device. The value of this coupling was taken to be 50 meV in most cases, as this was the value of the broadening of orbitals, due to the interaction with the electrodes, obtained from DFTB+[26] calculations.

This coupling value of 50 meV between the molecular orbitals and the electrodes was also used as the value for the broadening Δ_a in eqn (2). Note that this parameter describes the rate, at which electrons are transferred between different molecular orbitals, *i.e.* between different moieties or between the molecule and the electrodes, and thus is somewhat different than the coupling terms between neighboring atoms in tight-binding models. Due to the saturated (sp^3-hybridized) bridges, the moieties are relatively isolated from each other and from the electrodes, which explains why this value is significantly smaller than the values typically used to describe the coupling between orbitals on neighboring atoms in tight-binding models.

However, using this model it was determined that, in order for the unimolecular amplifier to work, the HOMO of the central moiety had to be coupled very weakly to the control electrode, otherwise the current through this junction would be similar to that through the other junctions, and thus the device would not produce much amplification. On the other hand, in order for the control electrode to affect the device *via* charging, the LUMO of the central moiety needed to be strongly coupled to this electrode. Therefore, for this device to work as a unimolecular amplifier, it was found that in the central moiety the HOMO must be relatively strongly coupled to the orbitals in the other moieties yet weakly coupled to the control electrode, while the LUMO must be relatively strongly coupled to the control electrode and weakly coupled to the other molecular orbitals. The different coupling strengths could possibly be obtained by choosing the acceptor moiety, so that the HOMO and LUMO had different symmetries, and so would interact differently with the electrode and the other moieties. For the purposes of the results calculated in the next section, the "strong" coupling value was set to 50 meV as described above, while the "weak" coupling value was set to 1 meV.

Three-terminal transport model results

As described below, the mechanism by which amplification occurred was found to be independent of the symmetry of the molecular device. Therefore, only the results obtained for the symmetric molecule UA6 of Fig. 3(b) will be shown, as these are somewhat easier to follow; results for the unsymmetrical UA5 were similar, with appropriate energy shifts, and somewhat noisier data.

We start by considering the case where only elastic transport is allowed. The currents through each molecule–electrode junction, I_L, I_C, and I_R, are plotted in Fig. 5(a) for the case where the bias on the central electrode is zero, $V_C = 0.0$ V. The corresponding energy of each of the molecular levels on each moiety is shown in Fig. 5(b). We will use the convention that positive current implies electrons entering molecule from the electrode through the relevant junction, and negative current implies electrons leaving the molecule. Note that the current between the left and the right electrodes only starts to increase sharply when $\varepsilon_{C,LUMO}$ approaches μ_C. Also, note that the current here is due to electrons being transmitted through the tails of the broadened molecular orbitals, as the levels remain quite far apart in energy over the entire bias range.

The current through the junction between the left electrode and the left part of the molecule, I_L, for different center voltages, V_C, is shown in Fig. 6(a), and the corresponding differential conductance dI_L/dV_{LR} is shown in Fig. 6(b). Increasing the bias on the center electrode V_C results in the peak in the current I_L occurring at a lower bias between the left and right electrodes.

Published on 06 June 2013. Downloaded by Osaka University on 25/06/2013 05:50:09.

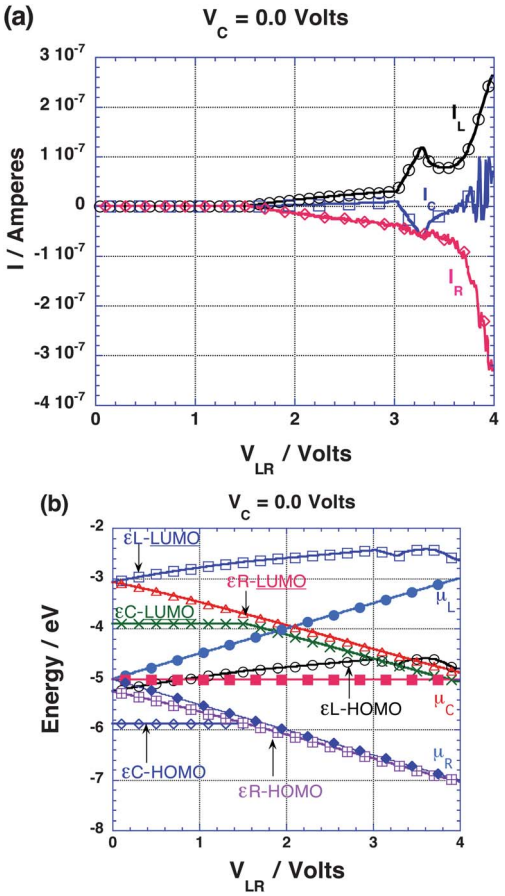

Fig. 5 (a) Currents for UA6 through each molecule–electrode junction, I_L, I_C, and I_R, as a function of the bias V_{LR} (0 to 4 volts) between the left and right electrodes, when the central electrode is at zero control bias ($V_C = 0$). (b) Energies of molecular levels $\varepsilon_{L,HOMO}$, $\varepsilon_{C,HOMO}$, $\varepsilon_{R,HOMO}$, $\varepsilon_{L,LUMO}$, $\varepsilon_{C,LUMO}$, and $\varepsilon_{R,LUMO}$ for the same V_{LR} range. The chemical potential of all electrodes starts at −5.0 eV at $V_{LR} = 0$.

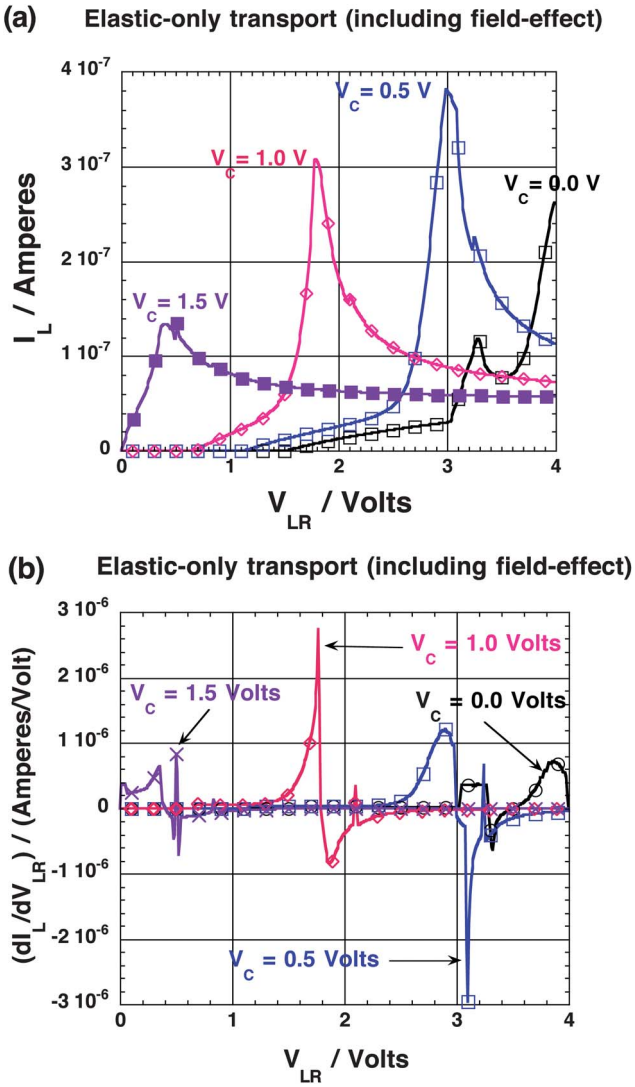

Fig. 6 (a) Current I_L and (b) differential conductance dI_L/dV_{LR} through the left part of molecule UA6, for different values of V_C, for elastic-only transport. The voltage on the *x*-axis V_{LR} is the bias between the left and right electrodes. Increasing the bias on the center electrode V_C results in the peak in the current I_L occurring at a lower value of V_{LR}.

To illustrate how the central voltage V_C affects the current between the left and right electrodes, the currents through each molecule–electrode junction, I_L, I_C, and I_R, as well as the corresponding energy and occupation of each of the molecular levels on each part of the molecule, are plotted in Fig. 7 for $V_C =$ 1.0 V. As the bias is increased, the energy and occupation of $\varepsilon_{R,HOMO}$ decrease. This results in charge being transferred from $\varepsilon_{C,HOMO}$, so that its occupation and energy also decrease. Due to the decrease in the total charge on the central moiety, $\varepsilon_{C,LUMO}$ also drops in energy, until it reaches μ_C, at which point it starts to charge. This results in both $\varepsilon_{C,HOMO}$ and $\varepsilon_{C,LUMO}$ remaining fixed in energy, as V_{LR} is increased further, but the continuing decrease in $\varepsilon_{R,HOMO}$ causes the occupation of $\varepsilon_{C,HOMO}$ to decrease further, effectively resulting in a rearrangement of the charge distribution within the central moiety. This decreased charge on $\varepsilon_{C,HOMO}$ allows charge from $\varepsilon_{L,HOMO}$ to transfer into it. Therefore, at this point, charge can flow through the molecule from the left to the right electrode, and there is an increase in the current. As the bias V_{LR} is increased even further, the energy of the orbitals in the left and right moieties continue to increase and decrease, respectively, due to the electric field and charging effects. Therefore, the levels in the different parts of the molecule move further apart, and the current decreases again, as the size of the overlap between the orbitals is decreased. Increasing the voltage applied to the central electrode, V_C, decreases the bias voltage V_{LR} at which this rearrangement of the charge on the central moiety occurs.

We now consider the situation where inelastic transport is also permitted. For simplicity, we consider the extreme case, where electrons can move into an orbital with lower energy at the same rate, at which they can move into an orbital with the same energy. This is done by removing the overlap term in eqn (11), so the rate at which the electrons can transfer between molecular orbitals is now independent of the difference in energy between the orbitals. However, it should be noted that eqn (4) and (5), which determine the charge, which each orbital tries to impose on the other orbitals, only allow for electron transfer from higher-energy orbitals to lower-energy ones. The results for the symmetric

 This journal is © The Royal Society of Chemistry 2013

Published on 06 June 2013. Downloaded by Osaka University on 25/06/2013 05:50:09.

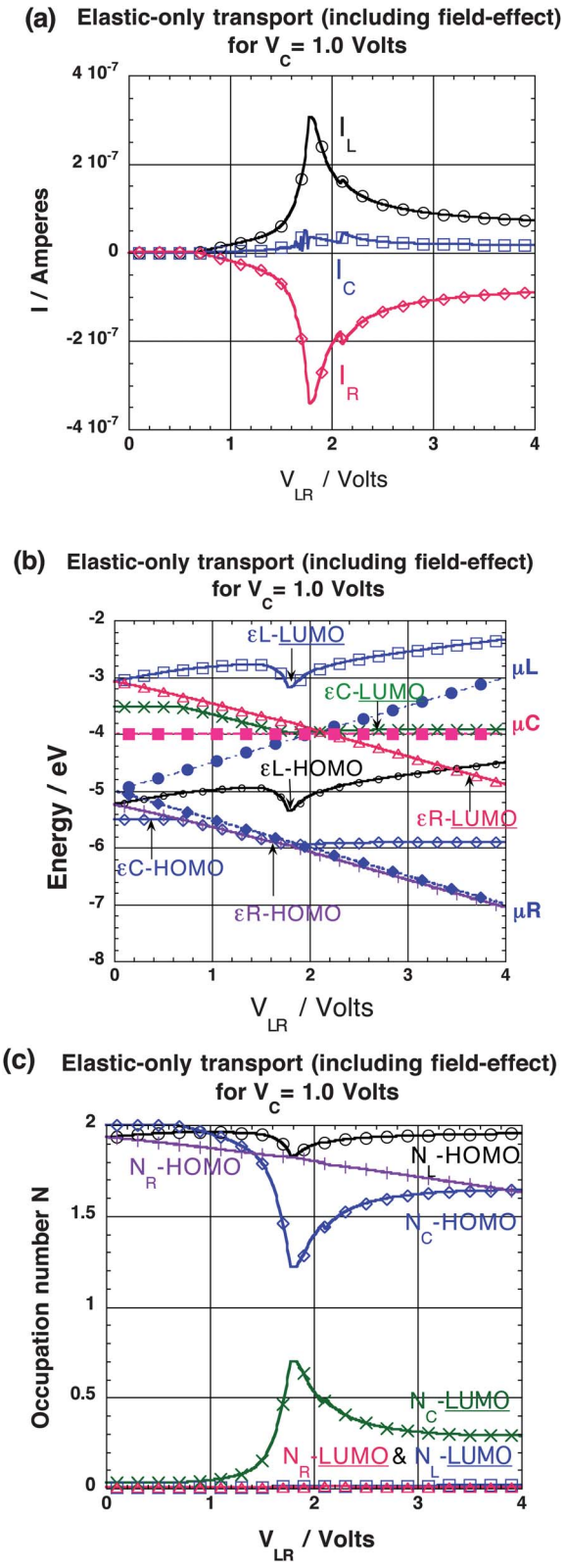

Fig. 7 (a) Currents through each molecule–electrode junction, I_L, I_C, and I_R, for V_C = 1.0 V for UA6. (b) Energies of molecular levels $\varepsilon_{L,HOMO}$, $\varepsilon_{C,HOMO}$, $\varepsilon_{R,HOMO}$, $\varepsilon_{L,LUMO}$, $\varepsilon_{C,LUMO}$, and $\varepsilon_{R,LUMO}$ for the same bias range. (c) Occupation of the molecular orbitals for the same bias range. At zero V_{LR}, the chemical potential of the electrodes is at −5.0 eV. The voltage on the *x*-axis V_{LR} is the bias between the left and right electrodes. The central voltage V_C changes the voltage at which the charge on the central moiety rearranges, shifting the peak in the current to lower bias.

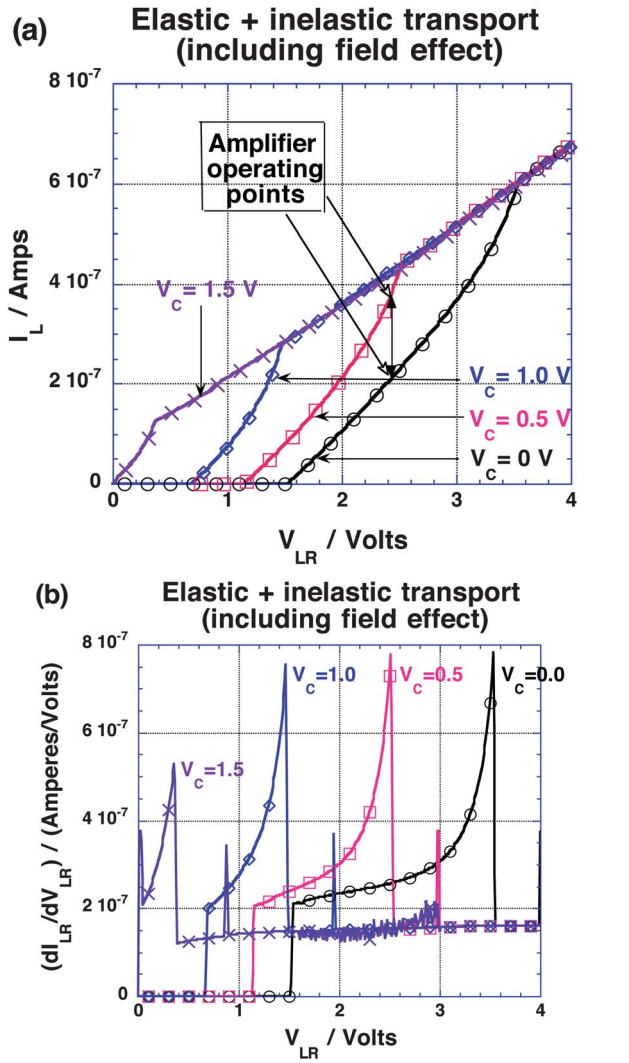

Fig. 8 (a) Current I_L and (b) differential conductance dI_L/dV_{LR} through left part of molecule UA6, for different values of V_C for the case where there is both elastic and inelastic transport through the molecule. The voltage on the *x*-axis V_{LR} is the bias between the left and right electrodes. Increasing the bias on the center electrode V_C results in the peak in the current I_L occurring at a lower value of V_{LR}.

molecule, where inelastic transport is allowed, are shown in Fig. 8. The current through the junction between the left electrode and the left part of the molecule, I_L, for different center voltages, V_C, is shown in Fig. 8(a); the corresponding differential conductance dI_L/dV_{LR} is shown in Fig. 8(b). As in the case of elastic-only transport, increasing the bias on the center electrode V_C results in the switching on of the current I_L occurring at a lower value of bias between the left and right electrodes V_{LR}.

The gradual displacement of the I_L currents with increasing control electrode voltage V_C seen in Fig. 8(a) is exactly what is needed to discuss molecule UA6 as a unimolecular amplifier (for vacuum-tube triodes the diode currents, quantified by Child's law,[48] are moved apart by retarding grid voltages[49]). For UA6 the separated I_L curves merge at higher currents, as the device enters into resonance independently of the control voltage V_C.

The open two-sided vertical arrow in Fig. 8(a) shows two points ("amplifier operating points") which could be used to

Published on 06 June 2013. Downloaded by Osaka University on 25/06/2013 05:50:09.

discuss power gain, one on the $V_C = 0$ curve ($V_{LR} = 2.4$ volts, $I_L = 2.02 \times 10^{-7}$ A) and the other at the $V_C = 0.5$ volt curve ($V_{LR} = 2.4$ volts, $I_L = 3.61 \times 10^{-7}$ A). If a load resistor of 1.0×10^7 Ω is placed in series between the L and R electrodes, then the voltage drop across them changes from $2.02 \times 10^{-7} \times 10^7 = 2.02$ volts to $3.61 \times 10^{-7} \times 10^7 = 3.61$: this is a change of 1.59 volts for a control potential change of only 0.5 volts: the amplification factor is $1.59/0.5 = 3.08$.

Details of how the central voltage V_C affects the currents are plotted in Fig. A of the ESI.†

The effect of the size of the HOMO–LUMO gap of the central moiety on the *I–V* characteristics was also investigated. Larger HOMO–LUMO gaps required a larger control bias V_C to be applied in order to bring the HOMO into resonance, so that the threshold voltage for the device to start to conduct was shifted to higher values. For very small HOMO–LUMO gaps, the LUMO becomes very close to the chemical potential of the central electrode, even for small values of V_C. This results in a large current through the central part of the molecule I_C, which dominates the total current at low bias.

Increasing all of the coupling strengths by a factor of 10 increases all the currents by the same factor, so that IV characteristics look qualitatively similar to the results presented above. However, increasing the strength of the coupling between the HOMO of the central moiety and the central electrode, $\Gamma_{CC,HOMO}$, by a factor of 10, relative to the other coupling strengths, causes the current from the central electrode to dominate for values of V_C of the order of 1.0 V, so that the device no longer functions as an amplifier. Therefore this coupling must be kept small, relative to the other values, so that $\Gamma_{CC,HOMO} = 0.001$ eV, *i.e.* about a factor of 50 smaller than the coupling between the other molecular levels and the electrodes. This small value keeps I_C much smaller than current through the other two molecule–electrode junctions, and thus is a necessary condition for this molecular device to operate as an amplifier.

The orbitals in the central moiety are shifted by the electric field (due to the bias applied to the electrodes) and also by the net charge on the molecule itself. Eliminating the electric field, by setting $U_{ja}^{ee} = 0.0$ eV, is shown in Fig. B of the ESI:† UA produces current amplification even in the absence of electric field effects on the molecular orbitals, demonstrating that it is not simply a field-effect transistor.

To construct a UA presents an interesting challenge for synthetic chemistry, as two orbitals on the same moiety have to interact differently with the electrode and/or with the orbitals in different moieties. One possible solution would be to design the molecule so that $\varepsilon_{C,HOMO}$ and $\varepsilon_{C,LUMO}$ have different symmetry, for example π-symmetry for $\varepsilon_{C,HOMO}$ and σ-symmetry for $\varepsilon_{C,LUMO}$. In that case, $\varepsilon_{C,HOMO}$ would interact more strongly with the π-symmetry orbitals on the other moieties, whereas $\varepsilon_{C,LUMO}$ would interact more strongly with the s-orbital of a metallic adatom on the electrode surface.

Conclusion

We have demonstrated how a unimolecular amplifier could be created, and explored the necessary electronic properties that it needs to function. In particular, a vital requirement is that the strength of the coupling between the HOMO of the central moiety and the central electrode should be much smaller than the coupling strengths between the other orbitals and the electrodes, otherwise the current through this junction will dominate the behavior of the device, so it will not behave as an amplifier.

In the case where only elastic transport occurs, the charge on the HOMO of the central moiety blocks the current from flowing through the device at low bias. As the bias is increased, $\varepsilon_{C,LUMO}$ drops in energy until it reaches μ_C, which then fixes the energy levels of the orbitals in the central moiety, and results in a rearrangement of the charge. This results in a decrease in the occupation of the HOMO, allowing a current to flow through the device. Increasing V_C decreases the bias V_{LR} at which this rearrangement occurs.

When inelastic transport is also allowed, the behavior is driven by a somewhat different mechanism. For values of V_C such that $\mu_C < \varepsilon_{C,LUMO}$, the charge on $\varepsilon_{C,HOMO}$ and the HOMO–LUMO gap of the central moiety prevent any current from flowing through the device. As V_C is increased, the energy levels of the central moiety are shifted upwards in energy, so that $\varepsilon_{C,HOMO}$ becomes available for transport at lower values of V_{LR}.

Thus, the transport behavior of this device can be controlled by changing the value of μ_C. Therefore, keeping the control electrode at a constant finite bias relative to the other electrodes (*e.g.* by using a material with a different work function), would render the device very sensitive to small voltage fluctuations on the control electrode, thus allowing it to amplify small signals.

We have also given two simple calculations of the amplification factor derivable from our calculated currents as a function of control bias.

Nevertheless, the relative simplicity of this model should be kept in consideration; many different effects, which are not included, could be important for device behavior. These include changes in the coupling parameters due to charging and applied electric fields, many-body and strong correlation effects, *etc.*

Acknowledgements

Funding by the European Union and the Free State of Saxony (ECEMP project A2 (EFRE) and ESF project 080942409 InnovaSens) is gratefully acknowledged. We also acknowledge support from the German Excellence Initiative *via* the Cluster of Excellence EXC 1056 "Center for Advancing Electronics Dresden" (cfAED), and partial support from the United States National Science Foundation (NSF-0848206). Computational resources were provided by the Center for Information Services and High Performance Computing (ZIH) in TU Dresden. One of us (RMM) is indebted to the Deutsche Forschungsgemeinschaft (DFG) for a Mercator Professorship. We thank Dmitry Ryndyk for a critical reading of this manuscript.

References

1 J. C. Cuevas and E. Scheer, *Molecular Electronics: an Introduction to Theory and Experiment*, World Scientific, Singapore, 2010.

 This journal is © The Royal Society of Chemistry 2013

Published on 06 June 2013. Downloaded by Osaka University on 25/06/2013 05:50:09.

2 A. Aviram and M. A. Ratner, Molecular Rectifiers, *Chem. Phys. Lett.*, 1974, **29**, 277–283.
3 R. M. Metzger, B. Chen, U. Höpfner, M. V. Lakshmikantham, D. Vuillaume, T. Kawai, X. Wu, H. Tachibana, T. V. Hughes, H. Sakurai, J. W. Baldwin, C. Hosch, M. P. Cava, L. Brehmer and G. J. Ashwell, Unimolecular Electrical Rectification in Hexadecylquinolinium Tricyanoquinodimethanide, *J. Am. Chem. Soc.*, 1997, **119**, 10455–10466.
4 M. Elbing, R. Ochs, M. Koentopp, M. Fischer, C. von Hänisch, F. Weigend, F. Evers, H. B. Weber and M. Mayor, A Single-Molecule Diode, *Proc. Natl. Acad. Sci. U. S. A.*, 2005, **102**, 8815–8820.
5 R. M. Metzger, Unimolecular Electrical Rectifiers, *Chem. Rev.*, 2003, **103**, 3803–3834.
6 R. M. Metzger, Unimolecular Electronics, *J. Mater. Chem.*, 2008, **18**, 4364–4396.
7 R. M. Metzger and D. L. Mattern, Unimolecular Electronic Devices, in *Unimolecular and Supramolecular Electronics II: Chemistry and Physics Meet at the Metal-Molecule Interface, Topics in Current Chemistry*, ed. R. M. Metzger, Springer, Heidelberg Dordrecht London New York, 2012, vol. 313, pp. 39–84.
8 S. Ami, M. Hliwa and C. Joachim, Molecular 'OR' and 'AND' Logic Gates Integrated in a Single Molecule, *Chem. Phys. Lett.*, 2003, **367**, 862–668.
9 R. M. Metzger, Unimolecular Rectifiers and Proposed Unimolecular Amplifier, *Ann. N. Y. Acad. Sci.*, 2003, **1006**, 252–276.
10 J. M. Thijssen and H. S. J. van der Zant, Charge Transport and Single-Electron Effects in Nanoscale Systems, *Phys. Status Solidi B*, 2008, **245**, 1455–1470.
11 K. K. Saha, B. K. Nikolic, V. Meunier, W. Lu and J. Bernholc, Quantum-Interference-Controlled Three-Terminal Molecular Transistors Based on a Single Ring-Shaped Molecule Connected to Graphene Nanoribbon Electrodes, *Phys. Rev. Lett.*, 2010, **105**, 236803.
12 R. Hoffmann, Interaction of Orbitals Through Space and Through Bonds, *Acc. Chem. Res.*, 1971, **4**, 1–9.
13 G. J. Ashwell, B. Ukrainska and W. D. Tirrell, Molecules that Mimic Schottky Diodes, *Phys. Chem. Chem. Phys.*, 2006, **8**, 3314–3319.
14 J. Lambe and R. C. Jaklevic, Molecular Vibration Spectra by Inelastic Electron Tunneling, *Phys. Rev.*, 1968, **165**, 821–832.
15 A. Honciuc, R. M. Metzger, A. Gong and C. W. Spangler, Elastic and Inelastic Electron Tunneling Spectroscopy of a New Rectifying Monolayer, *J. Am. Chem. Soc.*, 2007, **129**, 8310–8319.
16 U. Mazur and K. W. Hipps, Orbital-Mediated Tunneling, Inelastic Electron Tunneling, and Electrochemical Potentials for Metal Phthalocyanine Thin Films, *J. Phys. Chem. B*, 1999, **103**, 9721–9727.
17 J. Heurich, J. C. Cuevas, W. Wenzel and G. Schön, Electrical Transport through Single-Molecule Junctions: from Molecular Orbitals to Conduction Channels, *Phys. Rev. Lett.*, 2002, **88**, 256803.
18 C. J. Muller, J. M. van Ruitenbeek and L. J. de Jongh, Experimental Observation of the Transition from Weak Link to Tunnel Junction, *Physica C*, 1992, **191**, 485–504.
19 M. A. Reed, C. Zhou, C. J. Muller, T. P. Burgin and J. M. Tour, Conductance of a Molecular Junction, *Science*, 1997, **278**, 252–253.
20 J. Park, A. N. Pasupathy, J. I. Goldsmith, C. Chang, Y. Yaish, J. R. Petta, M. Rinkoski, J. P. Sethna, H. D. Abruña, P. L. McEuen and D. C. Ralph, Coulomb Blockade and the Kondo Effect in Single-Atom Transistors, *Nature*, 2002, **417**, 722–725.
21 B. Xu and N. J. Tao, Measurement of Single-Molecule Resistance by Repeated Formation of Molecular Junctions, *Science*, 2003, **301**, 1221–1223.
22 D. L. Lichtenberger, R. L. Johnston, K. Hinkelmann, T. Suzuki and F. Wudl, Relative Electron Donor Strengths of Tetrathiafulvene Derivatives: Effects of Chemical Substitutions and the Molecular Environment from a Combined Photoelectron and Electrochemical Study, *J. Am. Chem. Soc.*, 1990, **112**, 3302–3307.
23 M. E. Wacks, Electron-Impact Studies of Aromatic Hydrocarbons. II. Naphthacene, Naphthaphene, Chrysene, Triphenylene, and Pyrene, *J. Chem. Phys.*, 1964, **41**, 1661–1666.
24 In analogy to AA for TCNQ: (*a*) R. N. Compton and C. D. Cooper, Negative Ion Properties of Tetracyanoquinodimethan: Electron Affinity and Compound States, *J. Chem. Phys.*, 1977, **66**, 4325–4329; (*b*) S. H. Yang, C. L. Pettiette, J. Conceicão, O. Chesnovsky and R. E. Smalley, UPS of Buckminsterfullerene and Other Large Clusters of Carbon, *Chem. Phys. Lett.*, 1987, **139**, 233–238.
25 P. Kebarle and S. Chowdhury, Electron Affinities and Electron-Transfer Reactions, *Chem. Rev.*, 1987, **87**, 513–534.
26 D. Porezag, T. Frauenheim, T. Köhler, G. Seifert and R. Kaschner, Construction of Tight-Binding-like Potentials on the Basis of Density Functional Theory: Application to Carbon, *Phys. Rev. B: Condens. Matter Mater. Phys.*, 1995, **51**, 12947–12957.
27 M. Elstner, D. Porezag, G. Jungnickel, J. Elsner, K. Haugk, T. Frauenheim, S. Suhai and G. Seifert, Self-Consistent Charge-Density-Functional Tight-Binding Method for Simulations of Complex Materials Properties, *Phys. Rev. B: Condens. Matter Mater. Phys.*, 1998, **58**, 7260–7268.
28 T. Niehaus, M. Elstner, T. Frauenheim and S. Suhai, Application of an Approximate Density-Functional Method to Sulfur-Containing Compounds, *J. Mol. Struct.: THEOCHEM*, 2001, **541**, 185–194.
29 J. Soler, E. Artacho, J. Gale, A. García, J. Junquera, P. Ordejón and D. Sanchez-Portal, The SIESTA Method for *ab initio* Order-N Materials Simulation, *J. Phys.: Condens. Matter*, 2002, **14**, 2745–2779.
30 M. Paulsson, F. Zahid and S. Datta, Resistance of a Molecule, in *Handbook of Nanoscience, Engineering and Technology 12*, ed. W. A. Goddard, D. Brenner, S. E. Lyshevski and G. J. Iafrate, CRC Press, 2003, also available at cond-mat/0208183 2002.
31 R. Landauer, Spatial Variation of Currents and Fields Due to Localized Scatterers in Metallic Conduction, *IBM J. Res. Dev.*, 1957, **1**, 223–231.

Published on 06 June 2013. Downloaded by Osaka University on 25/06/2013 05:50:09.

32 M. Büttiker, Y. Imry, R. Landauer and S. Pinhas, Generalized Many-Channel Conductance Formula with Application to Small Rings, *Phys. Rev. B: Condens. Matter Mater. Phys.*, 1985, **31**, 6207–6215.
33 L. V. Keldysh, *Zh. Eksp. Teor. Fiz.*, 1964, **47**, 1515–1527; English translation: Diagram Technique for Non-Equilibrium Processes, *J. Exp. Theor. Phys.*, 1965, **20**, 1018–1026.
34 C. Caroli, R. Combescot, P. Nozières and D. Saint-James, Direct Calculation of the Tunneling Current, *J. Phys. C: Solid State Phys.*, 1971, **4**, 916–929.
35 K. Stokbro, J. Taylor and M. Brandbyge, Do Aviram-Ratner Diodes Rectify?, *J. Am. Chem. Soc.*, 2003, **125**, 3674–3675.
36 J. B. Pan, Z. H. Zhang, X. Q. Deng, M. Qiu and C. Guo, The Transport Properties of D-σ-A Molecules: A Strikingly Opposite Directional Rectification, *Appl. Phys. Lett.*, 2011, **98**, 013503.
37 J. B. Pan, Z. H. Zhang, X. Q. Deng, M. Qiu and C. Guo, Rectifying Performance of D-π-A Molecules Based on Cyanovinyl Aniline Derivatives, *Appl. Phys. Lett.*, 2010, **97**, 203104.
38 S. K. Yee, J. Sun, P. Darancet, T. D. Tilley, A. Majumdar, J. B. Neaton and R. A. Segelman, Inverse Rectification in Donor-Acceptor Molecular Heterojunctions, *ACS Nano*, 2011, **5**, 9256–9263.
39 H. Liu, N. Wang, P. Li, X. Yin, C. Yu, N. Gao and J. Zhao, Theoretical Investigation into Molecular Diodes Integrated in Series Using the Non-Equilibrium Green's Function Method, *Phys. Chem. Chem. Phys.*, 2011, **13**, 1301–1306.
40 M. Yu, N. Bovet, C. J. Satterly, S. Bengió, K. R. J. Lovelock, P. K. Milligan, R. G. Jones, D. P. Woodruff and V. Dhanak, *Phys. Rev. Lett.*, 2006, **97**, 166102.
41 P. Hohenberg and W. Kohn, Inhomogenous Electron Gas, *Phys. Rev.*, 1964, **136**, B864–B871.
42 W. Kohn and L. J. Sham, Self-Consistent Equations Including Exchange and Correlation Effects, *Phys. Rev.*, 1965, **140**, A1133–A1138.
43 J. P. Perdew, R. G. Parr, M. Levy and J. L. Balduz, Density Functional Theory for Fractional Particle Number: Derivative Discontinuities of the Energy, *Phys. Rev. Lett.*, 1982, **49**, 1691–1694.
44 J. P. Perdew and M. Levy, Physical Content of the Exact Kohn-Sham Orbital Energies: Band Gaps and Derivative Discontinuities, *Phys. Rev. Lett.*, 1983, **51**, 1884–1887.
45 J. P. Perdew and A. Zunger, Self-Interaction Correction to Density-Functional Approximations for Many-Electron Systems, *Phys. Rev. B: Condens. Matter Mater. Phys.*, 1981, **23**, 5048–5079.
46 A. J. Cohen, P. Mori-Sánchez and W. Yang, Insights into Current Limitations of Density Functional Theory, *Science*, 2008, **321**, 792–794.
47 G. C. Solomon, C. Herrmann and M. A. Ratner, Molecular Electronic Junction Transport: Some Pathways and Some Ideas, in *Unimolecular and Supramolecular Electronics II, Springer Top. Curr. Chem.*, ed. R. M. Metzger, Springer, Berlin Heidelberg, 2011, vol. 313, pp. 1–38.
48 C. D. Child, Discharge From Hot CaO, *Phys Rev.*, 1911, **32**, 492–511.
49 F. E. Terman, *Electronic and Radio Engineering*, McGraw-Hill, New York, NY, 4th edn, 1955, p. 183.

 This journal is © The Royal Society of Chemistry 2013